Clim Dyn (2008) 30:1–18
DOI 10.1007/s00382-007-0265-6

Closure of the Panama Seaway during the Pliocene: implications for climate and Northern Hemisphere glaciation

Daniel J. Lunt · Paul J. Valdes · Alan Haywood · Ian C. Rutt

Received: 17 October 2006 / Accepted: 10 April 2007 / Published online: 28 June 2007

Abstract The ''Panama Hypothesis'' states that the gradual closure of the Panama Seaway, between 13 million years ago (13 Ma) and 2.6 Ma, led to decreased mixing of Atlantic and Pacific water Masses, the formation of North Atlantic Deep water and strengthening of the Atlantic thermohaline circulation, increased temperatures and evaporation in the North Atlantic, increased precipitation in Northern Hemisphere (NH) high latitudes, culminating in the intensification of Northern Hemisphere Glaciation (NHG) during the Pliocene, 3.2–2.7 Ma. Here we test this hypothesis using a fully coupled, fully dynamic ocean-atmosphere general circulation model (GCM) with boundary conditions specific to the Pliocene, and a high resolution dynamic ice sheet model. We carry out two GCM simulations with ''closed'' and ''open'' Panama Seaways, and use the simulated climatologies to force the ice sheet model. We find that the models support the ''Panama Hypothesis'' in as much as the closure of the seaway results in a more intense Atlantic thermohaline circulation, enhanced precipitation over Greenland and North America, and ultimately larger ice sheets. However, the volume difference between the ice sheets in the ''closed'' and ''open'' configurations is small, equivalent to about 5 cm of sea level. We conclude that although the closure of the Panama Seaway may have slightly enhanced or advanced the onset of NHG, it was not a major forcing mechanism. Future work must fully couple the ice sheet model and GCM, and investigate the role of orbital and CO_2 effects in controlling NHG.

D. J. Lunt (✉) · P. J. Valdes · I. C. Rutt
School of Geographical Sciences, University of Bristol, University Road, Bristol BS8 1SS, UK
e-mail: d.j.lunt@bristol.ac.uk

D. J. Lunt · A. Haywood
Geological Sciences Division, British Antarctic Survey, High Cross, Madingley Road, Cambridge CB3 0ET, UK

Present Address:
A. Haywood
School of Earth and Environment, Environment Building, University of Leeds, Leeds LS2 9JT, UK

I. C. Rutt
Department of Geography, University of Wales Swansea, Singleton Park, Swansea SA2 8PP, UK

1 Introduction

Over the last 4 million years, Earth has experienced a transition from warmer climates to cooler climates, a change of about 3°C as an annual global mean (Haywood and Valdes 2004; Ravelo et al. 2004). Potential causes of Late Cenozoic Northern Hemisphere Glaciation (NHG) have been widely discussed (e.g. Raymo 1994; Rea et al. 1998; Maslin et al. 1998; Philander and Fedorov 2003; Ravelo et al. 2004, 2006; Bartoli et al. 2005; Barreiro et al. 2005; Fedorov et al. 2006). The final closure of the Panama Seaway, or formation of the 'Isthmus of Panama', has been proposed as a tectonically driven mechanism capable of intensifying NHG around 3 million years ago (3 Ma) (Keigwin 1982; Marshall et al. 1982; Bartoli et al. 2005). Although the actual timing and closure history of the Panama Seaway remains controversial (Haug and Tiedemann 1998 and references therein), its potential climatic effects have been demonstrated via a number of numerical modelling studies (e.g. Maier-Reimer et al. 1990; Mikolajewicz et al. 1993; Mikolajewicz and Crowley

1997; Murdock et al. 1997; Nisancioglu et al. 2003; Prange and Schulz 2004; Klocker et al. 2005; von der Heydt and Dijkstra 2005; Schneider and Schmittner 2006). These studies have linked the closure of the seaway to a reorganisation of ocean circulation, altered ocean heat transport and moisture fluxes to the Northern Hemisphere (NH), and changes to NHG. The influence that the closure of the seaway had on establishing a 'modern' ocean circulation in the North Atlantic, and in particular on the vigour of thermohaline circulation and North Atlantic Deep Water (NADW) formation, is a vital issue in this debate (e.g. Haug and Tiedemann 1998; Lear et al. 2003).

The majority of published modelling studies indicate that following a closure or restriction in the flow of surface waters through the Panama Seaway, the North Atlantic thermohaline circulation increases (e.g. Schneider and Schmittner 2006). This change relates to the cessation (or reduction) in the transport of fresh surface and sub surface waters from the Pacific into the Atlantic which reduces the buoyancy of North Atlantic surface waters leading to increased rates of NADW formation (Schneider and Schmittner 2006). This increase in NADW formation is associated with a strengthened flow of the western boundary currents in the North Atlantic (the Gulf Stream), and an increase in northward heat transports.

The ''Panama Hypothesis'', first proposed by Keigwin (1982), states that one of the effects of this change is to enhance evaporation rates in the North Atlantic, providing an enhanced moisture flux to northern high latitudes, increased precipitation, and an inception or intensification of NHG. However, the relative importance of increasing the northward transport of heat, which might act to delay the intensification of NHG, versus the increased moisture supply that facilitates the growth of the ice sheets, is largely unknown. One recent modelling study has suggested that perennial snow cover actually *decreased* in northern high latitudes when the seaway was closed (Klocker et al. 2005), casting doubt on the importance of the closure as a trigger for glaciation. Further questions have arisen over the moisture supply mechanism being capable on its own of intensifying NHG; some studies have suggested that it may have simply provided the necessary climatic preconditioning to facilitate ice sheet growth through variations in incoming solar radiation (e.g. Haug and Tiedemann 1998; Maslin et al. 1998).

Although considerable modelling effort has been focussed on establishing the impact of the seaway closure, the experiments carried out thus far have often used simplified representations of the atmosphere (e.g. Murdock et al. 1997; Klocker et al. 2005) and/or ocean bathymetry (e.g. von der Heydt and Dijkstra 2005), and/or ocean-only models (e.g. Nisancioglu 2003). Furthermore, nearly all of the experiments have been carried out using idealised boundary conditions or boundary conditions appropriate for the present-day and not the Pliocene. Finally, although Klocker et al. (2005) made predictions of NHG following closure of the seaway, their diagnostic was the GCM-predicted perennial snow cover, which has been shown to be a relatively poor indicator of glaciation, due to the low spatial resolution of the model, which neglects the important effects of sub-gridscale mountain ranges (Lunt et al. 2004). Until now, no study has attempted to incorporate a high resolution ice sheet modelling component.

In this study we present results from two Pliocene simulations in which the climatic impact of closing the Panama Seaway is explored. These simulations are carried out with a state-of-the-art fully coupled ocean-atmosphere GCM using a high-resolution three-dimensional representation of the atmosphere and oceans. The simulations are set up using a suite of Pliocene palaeoenvironmental boundary conditions derived from the PRISM2 digital data set (see Dowsett et al. 1999). Finally, we make a test of the ''Panama Hypothesis'' by using climatologies derived from the GCM simulations to force an offline ice sheet model, to predict the response of the Greenland and North American ice sheets to the seaway closure.

2 The models

2.1 The GCM: HadCM3

The particulars of the version of the UKMO GCM (hereafter referred to as HadCM3) used in this study are well documented (Gordon et al. 2000). In brief, HadCM3 was developed at the Hadley Centre for Climate Prediction and Research, which is a part of the UK Meteorological Office. The GCM consists of a coupled atmospheric model, ocean model and sea ice model. The horizontal resolution of the atmospheric model is 2.5° in latitude by 3.75° in longitude. This provides a grid spacing at the equator of 280 km in the north-south direction and 420 km east–west. The atmospheric model consists of 19 vertical layers. The spatial resolution in the ocean in HadCM3 is 1.25° × 1.25°, with 20 vertical layers. The atmospheric model has a time step of 30 min and includes a radiation scheme that can represent the effects of minor trace gases (Edwards and Slingo 1996). A parameterization of simple background aerosol climatology is also included (Cusack et al. 1998). The convection scheme used is that of Gregory et al. (1997). A land surface scheme includes the representation of the freezing and melting of soil moisture. The representation of evaporation includes the dependence of stomatal resistance on temperature, vapour pressure and CO_2 concentration (Cox et al. 1999). The ocean model uses the Gent-McWilliams mixing scheme (Gent and McWilliams 1990).

There is no explicit horizontal tracer diffusion in the model. The horizontal resolution allows the use of a smaller coefficient of horizontal momentum viscosity leading to an improved simulation of ocean velocities. The sea ice model uses a simple thermodynamic scheme and contains parameterisations of ice concentration (Hibler 1979) and ice drift and leads (Cattle and Crossley 1995). The model requires no surface energy or moisture flux corrections to be made, even for simulations of a thousand years or more (Gregory and Mitchell 1997).

2.2 The ice sheet model: GLIMMER

The 3D thermomechanical ice model used in this work was developed as part of the GENIE project (see http://www.genie.ac.uk) and is known as GLIMMER (Genie land ice model with multipy-enabled regions). The core of the model is based on the ice sheet model described by Payne (1999). The ice dynamics are represented with the widely used shallow-ice approximation, and a full three-dimensional thermodynamic model is used to determine the ice flow law parameter. The model is formulated on a Cartesian x–y grid, and takes as input the surface mass-balance and air temperature at each time step. In the present work, the ice dynamics time step is one year.

The main improvement made to the Payne (1999) model in the development of GLIMMER is the provision of a flexible coupling framework. The coupler is designed to allow easy coupling of the ice model to a global climate model, and allows several regional ice sheet models to be coupled simultaneously. To simulate the surface mass-balance, the present work uses the positive degree day (PDD) approach described by Reeh (1991). The basis of the PDD method is the assumption that the melt (w) that takes place at the surface of the ice sheet is proportional to the time-integrated temperature above freezing point, known as the positive degree day (units of time are days in this calculation):

$$w = \alpha \int_{\text{year}} \max(T(t), 0) dt, \tag{1}$$

where $T(t)$ is the surface air temperature and α is the PDD factor (a constant). This in turn relies on the assumption that the number of positive degree days is proportional to the energy availably for melting. The method described by Reeh (1991) and implemented here is somewhat more sophisticated, in that two PDD factors are used, one each for snow and ice, α_{snow} and α_{ice}, to take account of the different albedos and densities of these materials. In addition, a simple firn model represents the refreezing of snow as superimposed ice. The integral in Eq. (1) is calculated on the assumption of a sinusoidal annual variation in temperature, and takes as input the mean annual temperature and half-range. Diurnal and other variability is taken into account using a stochastic approach. This variability is assumed to have a normal distribution with a standard deviation of 5°C. The use of PDD mass-balance models is well established in coupled atmosphere-ice-sheet paleoclimate modelling studies (e.g. DeConto and Pollard 2003).

GLIMMER includes a representation of the isostatic response of the lithosphere, which is assumed to behave elastically, based on the model of Lambeck and Nakiboglu (1980). The timescale for this response is 3,000 years. In all model runs described below, the isostasy model is initialised on the assumption that the present-day bedrock depression is in equilibrium with the ice sheet load.

In the present work, the GLIMMER bedrock topography is derived from two sources. For Greenland, we use the digital elevation model (DEM) compiled by Bamber et al. (2001a, b) with the resolution of the data reduced from 5 to 20 km by areal averaging. For North America, we use the ETOPO2 dataset (US Department of Commerce et al. 2001), transformed by areal averaging to a grid based on a stereographic projection centred at 62°N 97°W.

The forcing data from HadCM3 are transformed onto the ice model grid using bilinear interpolation, which ensures that precipitation is conserved in the atmosphere-ice-sheet coupling. In the case of the surface air temperature field, a vertical lapse-rate correction is used to take account of the difference between the high-resolution topography seen within GLIMMER, and that represented with HadCM3. If the HadCM3 temperature is denoted T_E, and the temperature on the GLIMMER grid is T_G, then the lapse-rate correction may be written:

$$T_G = T_E + \alpha_E h_E - \alpha_G h_G, \tag{2}$$

where h_E is the height of the HadCM3 topography, h_G is the height of the GLIMMER topography, and α_E and α_G being lapse-rates. In the present work, $\alpha_E = \alpha_G = 8.0$ K km^{-1}. Due to the non-linear nature of the PDD mass balance, the application of a lapse-rate correction to surface air temperature means that energy may not be conserved in the coupling. However, the PDD mass-balance scheme is not based on an explicit energy calculation, but depends on the local surface temperature as a proxy for available energy. The use of a lapse-rate correction to better represent the local temperature is established in previous work (e.g. Pollard and Thompson 1997). The value of the lapse-rate, 8.0 K km^{-1}, is in line with the more recent work by Hanna et al. (2006), and is also consistent with work by Huybrechts (1996), where the analytically-defined temperature climatology was based on surface observations. However, in the pre-industrial HadCM3 simulation, the

lapse-rate is 5.6 K km^{-1} in the mid-troposphere, although this does vary significantly with height.

3 Experimental design

Two Pliocene coupled ocean-atmosphere simulations are carried out, both of which represent continuations of the simulation presented in Haywood and Valdes (2004). Our control Pliocene simulation with a closed seaway (hereafter referred to as $Plio^{CS}$) is equivalent to the Pliocene simulation of Haywood and Valdes (2004). It was set up with Pliocene boundary conditions derived from the United States Geological Survey (USGS) PRISM2 digital data set. The particulars of the PRISM2 data set have been well documented in previous papers (Dowsett et al. 1999; Haywood et al. 2000 and references therein). In brief, the prescribed boundary conditions cover the time slab between 3.29 and 2.97 Ma according to the geomagnetic polarity time scale (Berggren et al. 1995). Boundary conditions integrated into the model that are specific to the Pliocene include: (1) continental configuration, modified by a 25-m increase in global sea level, (2) modified present-day elevations, (3) reduced ice sheet size and height for Greenland (about 50% reduction) and Antarctica (about 33% reduction), and (4) Pliocene vegetation distribution. The geographical extent of the Greenland and Antarctic ice sheets within the PRISM2 data set was based on global sea-level estimates derived for the Pliocene by Dowsett and Cronin (1990). The PRISM2 reconstruction uses model results from Michael Prentice (personal communication from Harry Dowsett; cited in Dowsett et al. (1999)) to guide the areal and topographic distribution of Antarctic and Greenland ice. A 25-m sea level rise is equivalent to a maximum decrease in global average salinity of approximately 0.25 psu, which is small and therefore was not included in our Pliocene coupled simulations. For a more detailed description of the PRISM2 data set and how it differs from earlier PRISM data sets see Dowsett et al. (1999: http://pubs.usgs.gov/of/1999/of99-535/).

We also present results from a Pliocene sensitivity experiment (hereafter referred to as $Plio^{OS}$), where the Panama Seaway is specified as being open. This was achieved by modifying the land sea mask and ocean bathymetry in the Panama Seaway region by removing 3 land grid boxes and by replacing them with 18 ocean grid boxes approximately 370 m deep. This depth is chosen primarily because it is consistent with the bathymetry in the region adjacent to the seaway—deepening the seaway further would require deepening of additional ocean gridboxes in order to obtain a realistic bathymetry. Comparison with indicators of the closure history from marine and terrestrial data (Schmidt 2007) suggests that our $Plio^{OS}$ simulation pertains to a period approximately 6–13 Ma, although our purpose is not primarily to simulate a particular time period, but to carry out a sensitivity study to the closure of the seaway. The local ocean bathymetry in the $Plio^{CS}$ and $Plio^{OS}$ simulations is shown in Fig. 1. In addition, in the $Plio^{OS}$ simulation we define South America as an island for the barotropic stream-function calculation; otherwise, the integrated flow around South America would be constrained to be zero, which could lead to unrealistic flow through the seaway. All other boundary conditions in the two simulations are identical.

A CO_2 concentration of 400 ppmv is used in both simulations. This is a justifiable value when available proxy estimates of Pliocene atmospheric CO_2 concentrations are considered. Estimates have been derived from the analysis of stomatal density of fossil leaves (Van der Burgh et al. 1993; Kürschner et al. 1996), through analyses of $\delta^{13}C$ ratios of marine organic carbon (Raymo et al. 1996) and through measurement of the differences between the carbon isotope composition of surface and deep waters (Shackleton et al. 1992). All three proxy methods suggest that absolute CO_2 levels during the time period range from

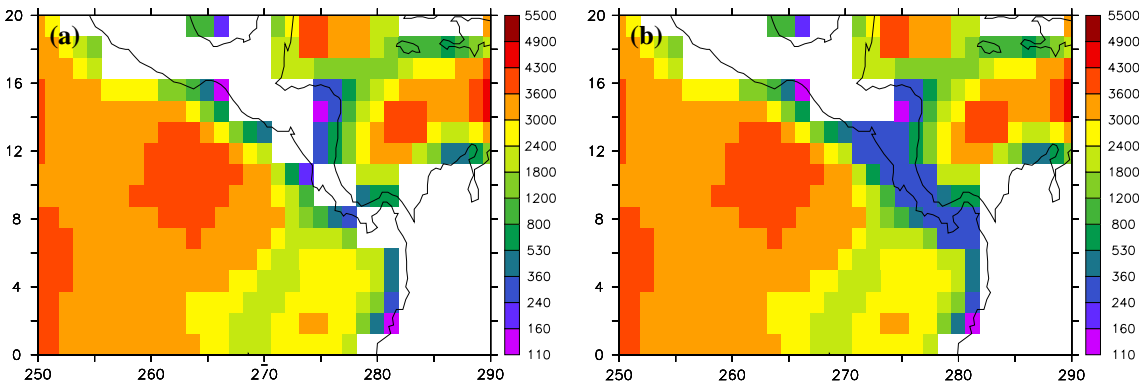

Fig. 1 Bathymetry in Panamanian region in the **a** $Plio^{CS}$ and **b** $Plio^{OS}$ GCM simulations, [m]

Table 1 Summary of GCM simulations

Model simulation	pCO_2 (ppm)	Radiation balance at the TOA (W m^{-2})	Length of simulation (years)	Climatological means (years)	Global average surface temperature (°C)
Pre-industrial	280	–0.23	753	33	14.0
$Plio^{CS}$	400	0.21	300 + 263	43	17.1
$Plio^{OS}$	400	0.28	300 + 249	29	16.8

360 to 400 ppmv, compared to mid-nineteenth century levels of approximately 280 ppmv and modern concentrations of 378 ppmv. For a summary of the experimental design see Table 1.

Both the $Plio^{CS}$ and $Plio^{OS}$ simulations were continued from the end of the Pliocene simulation presented in Haywood and Valdes (2004). Simulation $Plio^{CS}$ was integrated for 263 years, bringing the total integration length to over 500 years. Climatological means were derived from the last 43 years of the run. Simulation $Plio^{OS}$ was integrated for a further 249 years with the final 29 years used to derive the climatological means. All the model results from our $Plio^{CS}$ and $Plio^{OS}$ simulations, including many variables not directly discussed in this paper, and including seasonal variability, are available online, at http://www.bridge.bris.ac.uk/resources/simulations. A username and password are available on request from the corresponding author. An analysis of the model's energy imbalance at the top of the atmosphere (TOA) for all simulations is presented in Table 1. For both simulations the trend in global mean surface air temperatures over the final 50 years of integration is small (0.12°C $century^{-1}$ for the $Plio^{CS}$ case and 0.05°C $century^{-1}$ for the $Plio^{OS}$ case). Therefore, we consider that both of the model runs have reached a quasi-equilibrium state. Further discussion of the degree of equilibrium of the simulations can be found in Sect. 6.

For the ice sheet model simulations, we use the GCM-predicted climatological monthly mean surface air temperature and precipitation to force GLIMMER. We do not use the anomaly method (e.g. Lunt et al. 2004) as this is inappropriate for climates, such as these, which are considerably different from modern. We run GLIMMER for 20,000 years, initialised from the modern observed ice sheet and bedrock geometry (Bamber et al. 2001a, b). Because the ice sheet is run off-line, we neglect any feedbacks between the ice sheet and the climate due to changes in the albedo of the ice sheet. Atmospheric circulation changes caused by changes in ice sheet geometry are also ignored. However, the use of a vertical lapse-rate correction in transforming the HadCM3 climate to the GLIMMER grid does represent the local aspect of the ice elevation feedback.

4 GCM results

The Closed Seaway ($Plio^{CS}$) simulation has been evaluated in some detail by Haywood and Valdes (2004) and Haywood et al. (2005). As explained in Sect. 3, the $Plio^{CS}$ simulation used in this paper is actually a continuation of the Haywood and Valdes (2004) Pliocene simulation, and there are no important differences between them. They found their Pliocene simulation to agree reasonably well with the available data, in particular when updated tropical SST records were incorporated into the comparison (Haywood et al. 2005). In brief, there was a 3.1°C increase in global annual mean surface air temperature relative to a comparable pre-industrial simulation. The regional and seasonal patterns of temperature and precipitation change were qualitatively similar to those predicted for future climate change over the next century (IPCC 2001), showing, for example, greatest warming at the poles and over continents, with relatively little temperature change over the Southern Ocean. They found that neither the oceanic or atmospheric heat transports were greatly modified relative to pre-industrial, and that the surface temperature increases were primarily driven by the elevated pCO_2 concentration and the lower ice sheets, and were amplified by cloud and albedo feedbacks.

The difference in annual mean surface air temperature between our $Plio^{CS}$ and $Plio^{OS}$ simulations is shown in Fig. 2. Throughout this paper, we present anomalies as $Plio^{CS}$–$Plio^{OS}$; i.e. we plot the effect of *closing* the seaway, as this is most appropriate to the ''Panama Hypothesis'' being tested, and is consistent with previous work (e.g. Klocker et al. 2005). It is clear that the response to the closure of the seaway is in general bipolar, with warming in the NH and cooling in the Southern Hemisphere (SH). The maximum warming, of about 7°C, occurs in the North Atlantic. However, the global annual mean change is small, only +0.25°C, consistent with the idea that the primary response of the system is a reorganisation of the ocean circulation. There is not a large seasonal signal in the temperature response; the bipolar structure persists with a similar magnitude throughout the year.

In order to diagnose this response, we turn first to the zonal mean heat transports of the coupled system.

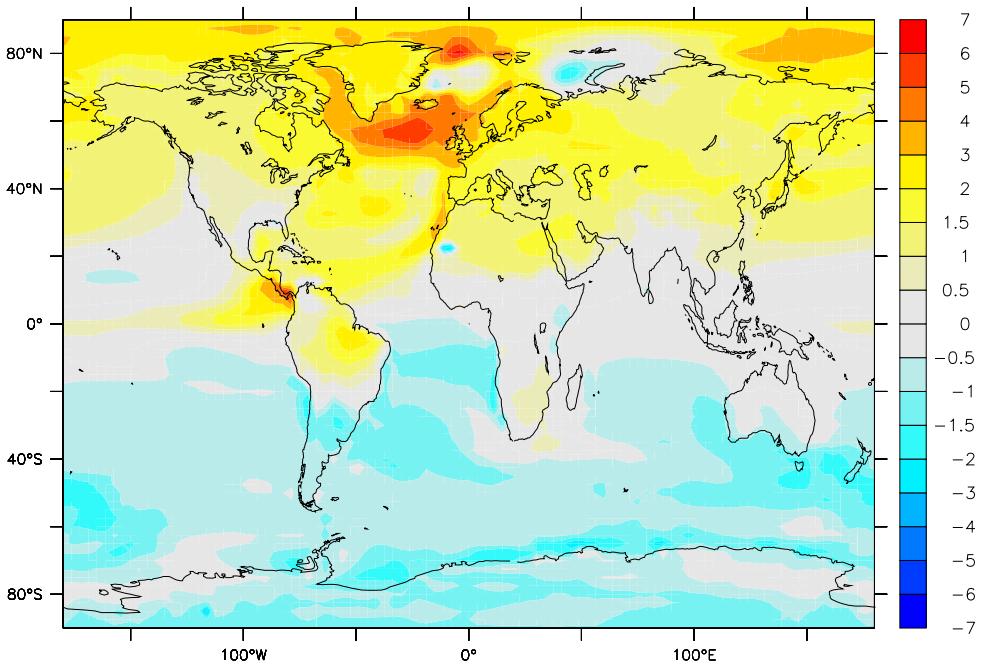

Fig. 2 Surface temperature change, $Plio^{CS}$–$Plio^{OS}$ (K)

Figure 3a shows the northward heat transport in the $Plio^{CS}$ simulation, separated into the atmosphere, ocean, and total components. The heat transports are qualitatively similar to those from a pre-industrial control simulation, which is in good agreement with observations (Peixoto and Oort 1992) for the total heat transport, but the ocean does not in general transport enough heat in either hemisphere, and the atmosphere transports too much heat. Figure 3b shows the change in this northward heat transport, $Plio^{CS}$–$Plio^{OS}$, also for the ocean, atmosphere, and total. It shows that the atmosphere and ocean respond in opposite ways to the closure of the seaway, with the ocean transporting more heat polewards in the NH, and less heat polewards in the SH, and the atmosphere transporting less heat polewards in the NH, and more heat polewards in the SH. By reference to Fig. 2, it is clear that it is the changes to the *ocean* heat transports which dominate at the surface, resulting in the bipolar response. The ocean heat transports can be further partitioned into their separate basins. Figure 3c shows the heat transport change as before, but for the Pacific and Atlantic basins separately (changes in the Indian Ocean are small in comparison). This indicates that the changes in the Pacific are opposite to the changes in the Atlantic, but again, reference to Fig. 2 shows that in global terms it is the Atlantic changes which dominate. Figure 3d shows the heat transports in the $Plio^{CS}$ and $Plio^{OS}$ simulations separately, for the Atlantic and Pacific. It shows that in the SH the Atlantic moves from a poleward-transporting regime with an open seaway to a northward-transporting regime with a closed seaway. The Pacific basin is poleward transporting in both simulations, but changes its relative intensity in both hemispheres upon closure of the seaway. One further diagnostic can be assessed—the relative contribution of the zonally symmetric ('overturning') and non zonally-symmetric ('gyre') components of the heat transports (Bryan 1969). These are shown in Fig. 3e for the dominating Atlantic basin alone; it is the overturning component which is the most important. This can also be illustrated in terms of the meridional overturning circulation (MOC) in the Atlantic in the two cases (Fig. 4). This shows the dramatic difference in MOC in the two cases—from the weakly overturning MOC in the open seaway case to the more strongly overturning MOC, similar to pre-industrial, in the closed seaway case. In summary, we have shown that the bipolar response to the closure of the Panama Seaway, with warming in the NH and cooling in the SH, is driven primarily by changes in overturning in the Atlantic basin, which changes regime from poleward-transporting, weak overturning in the $Plio^{OS}$ simulation to northward-transporting, strong overturning in the $Plio^{CS}$ simulation. Previous workers have found similar changes to heat transports (e.g Prange et al. 2006) and Atlantic overturning (e.g. Schneider and Schmittner 2006), but these have not always resulted in such a bipolar response in terms of surface temperature change (e.g. Murdock et al. 1997). This is probably related to the fact that these models have often used energy-moisture balance atmospheres, which fail to transport the surface temperature anomalies sufficiently in the zonal direction.

In order to further understand this change in circulation regime, we examine first the change in latent cooling of the oceans (proportional to evaporation in seaice-free regions).

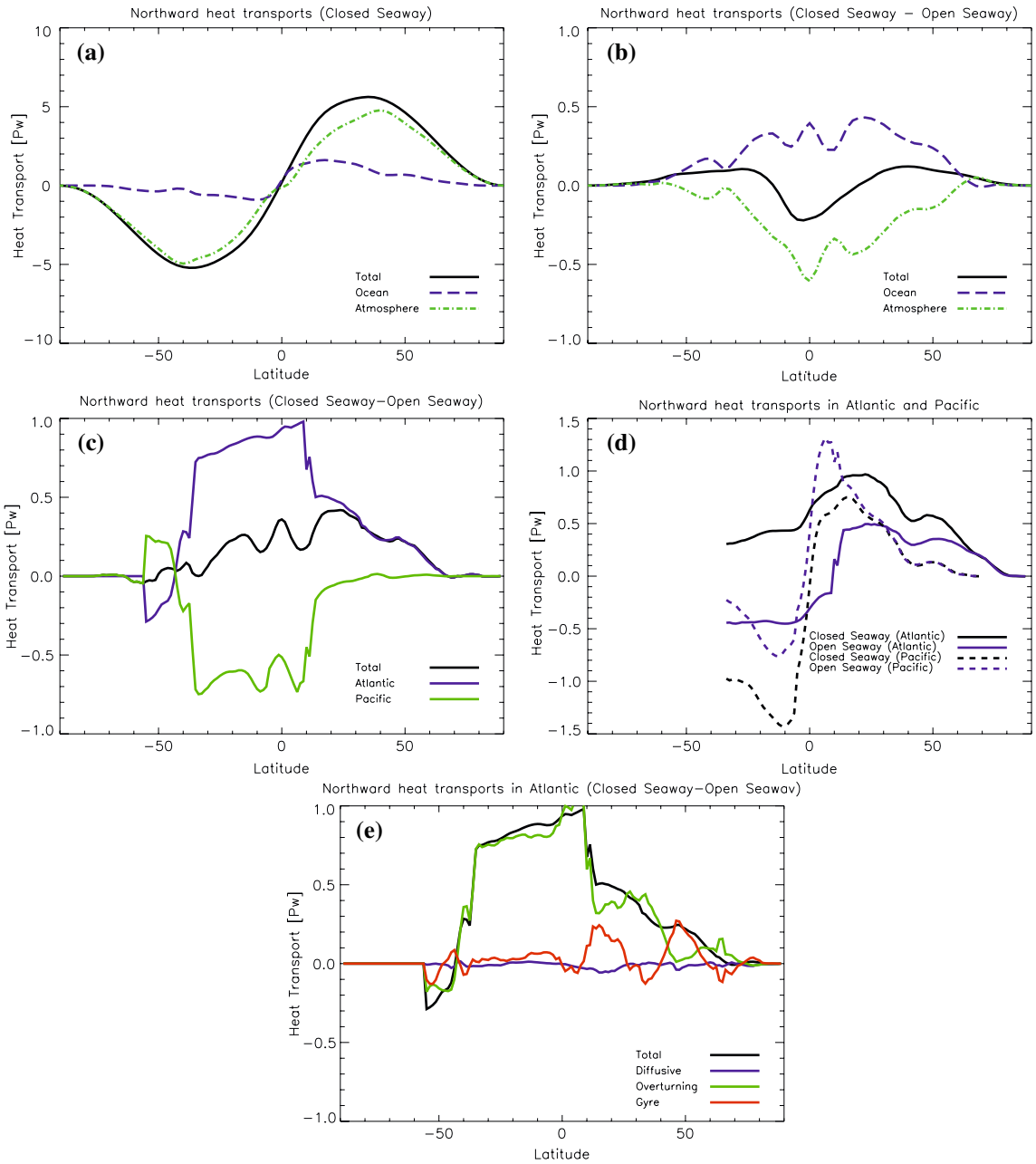

Fig. 3 Northward heat transports, [PW]. **a** Plio^{CS}, partitioned into atmosphere, ocean, and total. **b** Plio^{CS}–Plio^{OS}, partitioned into atmosphere, ocean, and total. **c** Plio^{CS}–Plio^{OS} ocean transports, partitioned into basins. **d** Plio^{CS} and Plio^{OS} ocean transports, partitioned into basins. **e** Plio^{CS}–Plio^{OS} Atlantic ocean transports, partitioned into type

This is illustrated in Fig. 5. It shows that in the North Atlantic, there is a large increase in evaporation in the Plio^{CS} simulation, relative to the Plio^{OS}. It is likely that this is associated with the increased temperatures in this region (Fig. 2). There is a corresponding decrease in evaporation in the South Atlantic. This leads to a change in the surface salinity, shown in Fig. 6a. Unsurprisingly, this is strongly correlated with the change in evaporation, in particular in the North Atlantic. In the mid ocean (450 m depth, Fig. 6b), there is a similar change in salinity as at the surface, but it is more diffuse, and there is a strong local signal in the Caribbean region. This local signal is directly related to the closure of the seaway, and the local changes in ocean circulation which subsequently occur. Figure 7 shows the ocean surface velocity in the Panama region in the Plio^{OS} simulation. The surface flow through the strait is dominated by the surface winds, in particular the trade wind easterlies. Figure 8 shows the vertical structure of the flow through the seaway. In the zonal direction, the surface winds influence the flow down to the bottom of the seaway,

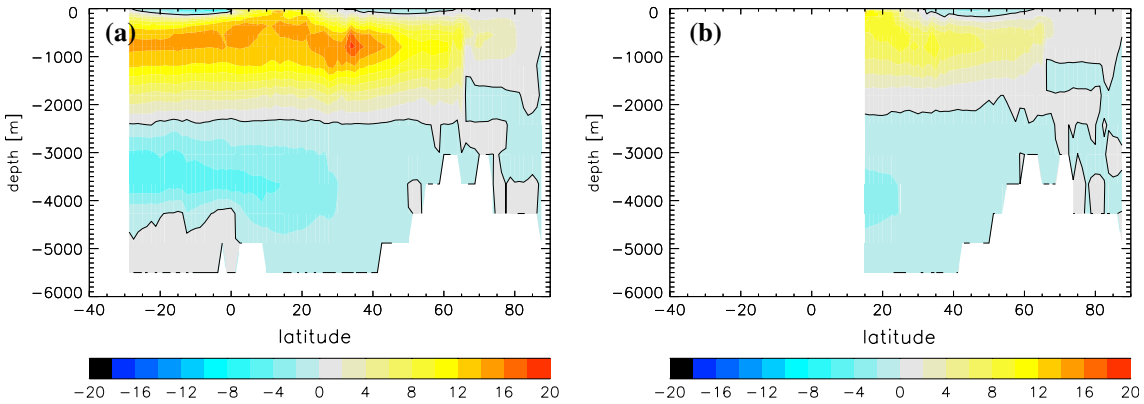

Fig. 4 Meridional overturning streamfunction, $\psi(y,z) = -\int_{-h}^{z}\int_{x_1}^{x_2} v(x,y,z)dxdz$, in the Atlantic in **a** Plio^{CS} and **b** Plio^{OS} (Sv). x_1 and x_2 are the western and eastern boundaries of the basin respectively, h is the depth of the ocean floor, and v is the meridional velocity. The integral is only shown in enclosed basins, where the divergence of the flow is zero

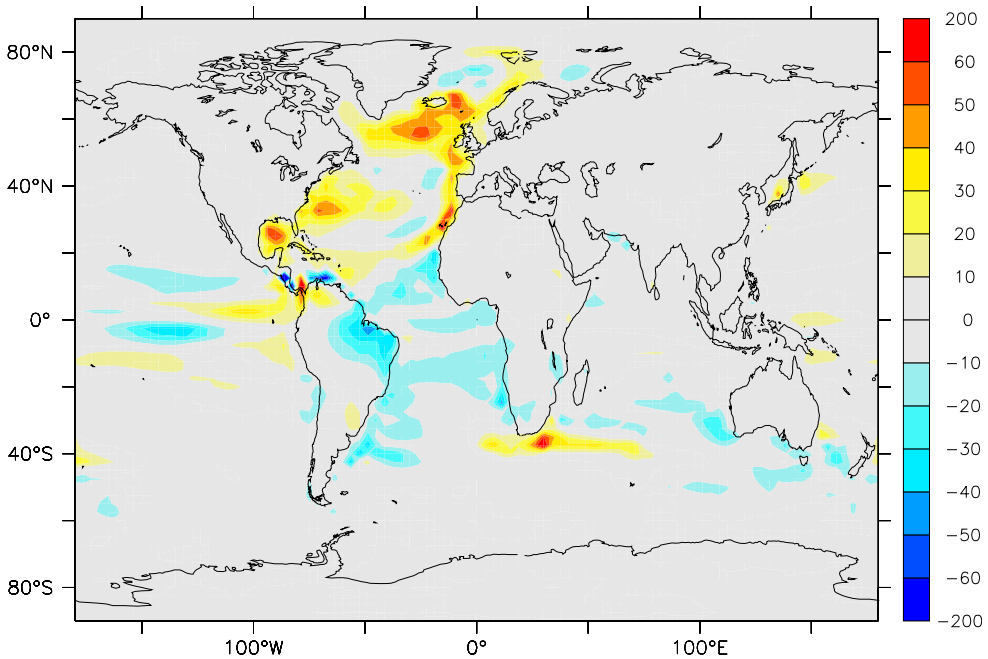

Fig. 5 Latent heat at surface, Plio^{CS}–Plio^{OS} (Wm^{-2}). Positive upwards, i.e. positive values represent increased evaporation in the Plio^{CS} case

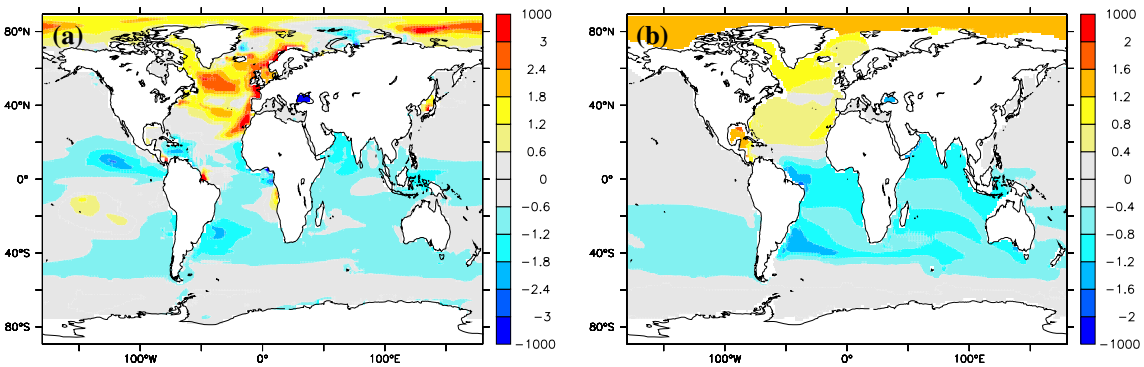

Fig. 6 Salinity, Plio^{CS}–Plio^{OS} (psu). **a** at the surface, and **b** at a depth of 450 m

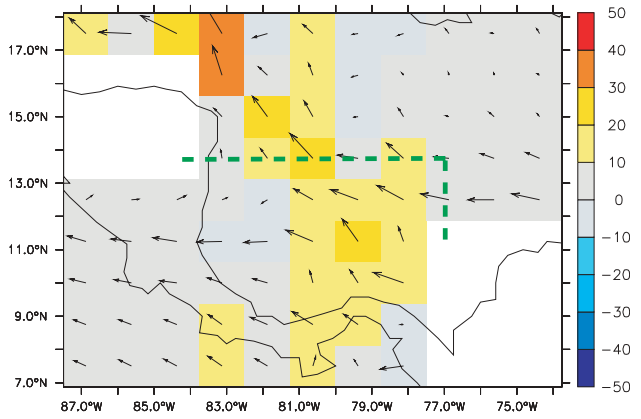

Fig. 7 Flow (cm/s) at the surface. *Coloured shading* is the meridional component. *Dotted green lines* are the cross sections shown in Fig. 8

whereas in the meridional direction, there is a significant return flow at depth. Because of the west-east orientation of the seaway, it is the meridional flow which dominates the total mass transport; the transport through the cross sections in Fig. 8 being 9.6 Sv meridionally from Pacific to Atlantic, and 1.6 Sv zonally from Atlantic to the Pacific. This partitioning is dependent on the definition of the cross sections, but the net flow through the seaway, 8.0 Sv from Pacific to Atlantic, is not (due to continuity of the incompressible fluid, and the lack of significant horizontal recirculation in the seaway). This value is consistent with the study of Schneider and Schmittner (2006), who found a Pacific to Atlantic throughflow of 10 Sv with a 700 m sill, and 5 Sv with a 130 m sill. The significant Pacific-Atlantic mass flux results in a weaker salinity gradient between the two basins than in the Plio^{CS} simulation. The absence of very saline waters in the Atlantic results in a weaker MOC, which in turn leads to cooler high-latitude Atlantic surface water masses, and less evaporation, thereby further weakening the original cross-basin salinity contrast. Again, these findings, including the magnitude of the flow through the seaway, are consistent with those of previous workers.

Also of interest, especially for the ice sheet model simulations which follow, are the changes to precipitation. The precipitation change, Plio^{CS}–Plio^{OS}, is shown in Fig. 9. This shows that the closure of the seaway ultimately results in an increase in precipitation over much of the NH, associated with the increased SSTs. Of particular interest is the increase in precipitation over Greenland, especially the east coast. This increase persists through most of the year, but is not present in May and June. There is also an increase in precipitation over the high latitudes of North America, but this is significantly smaller in magnitude than over Greenland.

In summary, the GCM results fully support the first part of the ‘‘Panama Hypothesis’’, with the closure of the Panama Seaway leading to a greater salinity contrast between the Pacific and Atlantic basins, a resulting increase in the strength of the Atlantic MOC, leading to warmer and more evaporative waters at high latitudes, and ultimately increased precipitation in NH high latitudes. The question which we now address is which of the two factors, warmer temperatures or increased precipitation, have the greatest effect on NHG; in other words, is the second part of the ‘‘Panama Hypothesis’’ correct, and to what extent.

5 Ice sheet model results

Because GLIMMER is a relatively new model, and has never previously been forced with output from the HadCM3 GCM, it is necessary to carry out an initial assessment of the

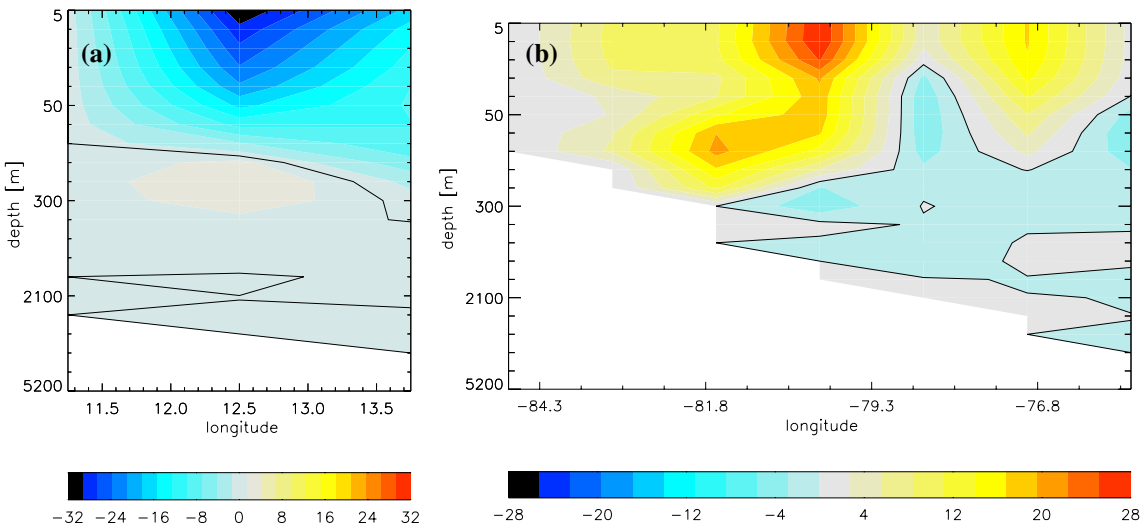

Fig. 8 Vertical structure of flow (cm/s) through the seaway in the **a** zonal and **b** meridional directions, through the sections shown in Fig. 7

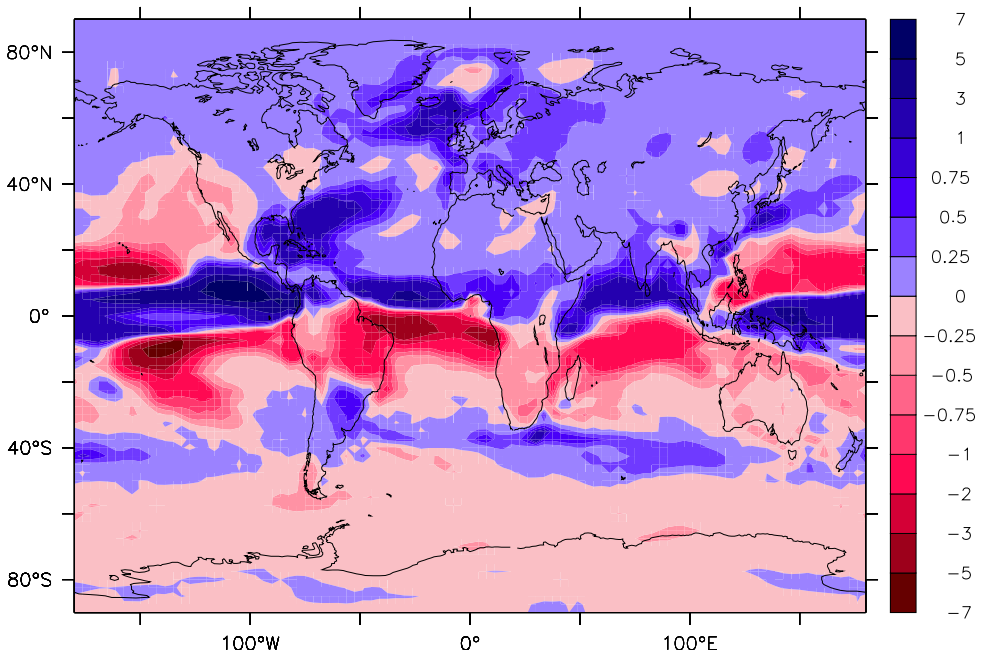

Fig. 9 Precipitation change, Closed Seaway–Open Seaway (mm/day)

sensitivities of the model. We do this by attempting to simulate the pre-industrial Greenland ice sheet. We use a HadCM3 pre-industrial simulation, spun up for nearly 1,000 years (the simulation is in fact a continuation of the pre-industrial simulation used in Haywood and Valdes 2004). We take the temperature and precipitation monthly-mean climatologies from the last 33 years of this GCM simulation, and use them to force the GLIMMER ice sheet model, over the Greenland region, for 20,000 years. Our initial condition is the present-day observed Greenland ice sheet (Bamber et al. 2001a, b). For this study, we focus on the sensitivity to the PDD factors, α_{snow} and α_{ice}, described in Sect. 2. We carry out 4 simulations, *low*, *medium*, *high*, and *very high*, with corresponding increasing values of α_{snow} and α_{ice}, as summarised in Table 2. The higher the PDD factor, the greater the amount of melt given a certain temperature above freezing. The resulting equilibrium ice sheet geometries predicted by GLIMMER are shown in Fig. 10, along with the observed present-day ice sheet (considered the 'goal' of the the ice sheet simulations; the difference between the present-day and pre-industrial Greenland ice sheet is likely to be small in the context of typical ice sheet timescales). This shows that only the 'collapsed' *very high* simulation can be immediately discounted. The other simulations all result in ice sheets which are qualitatively similar to the observed ice sheet, but which are too shallow at the centre, and too extensive at the margins. In addition, the simulated ice sheet has a predominantly marine margin, whereas the real ice sheet margin is mostly inland. This means the geometry of the ice sheet is being controlled by the simulated marine ice calving processes, rather than the ablation that would be dominant on an inland margin. However, the fact that important drainage processes (ice streams) are unrepresented in GLIMMER, due to limitations of the dynamics formulation and insufficient horizontal resolution, means that it is probably unreasonable to expect the ice sheet geometry to be more realistic than this. The total ice volumes in terms of equivalent sea level (calculated assuming a linear relationship, a global ocean area of 361×10^6 km^2, and an ice density of 910 kg m^{-2}), are 9.9, 9.5, 8.9, and 1.5 m for the *low*, *medium*, *high*, and *very high* simulations respectively, compared to the observed 7.3 m (all equivalent sea levels are summarised in Table 3). In addition to having the most realistic total ice volume, the *high* simulation also has the most realistic ice sheet extent, in particular in the west coast of Greenland. Further sensitivity studies (not shown) show that the bifurcation point between collapsed and non-collapsed ice sheets lies between PDD factors of $\alpha_{snow} = 0.019$ and $\alpha_{snow} = 0.024$ (with corresponding values for α_{ice}); so reference to Table 2 shows that the *high* simulation is not particularly close to collapsing. Although the simulated ice sheets are not perfect, they compare well with results obtained using observed forcing climatologies (A.J. Payne, University of Bristol, personal communication).

Table 2 Summary of PDD factor simulations

PDD factor	α_{snow}	α_{ice}
Low	0.003	0.008
Medium	0.006	0.016
High	0.012	0.032
Very high	0.024	0.064

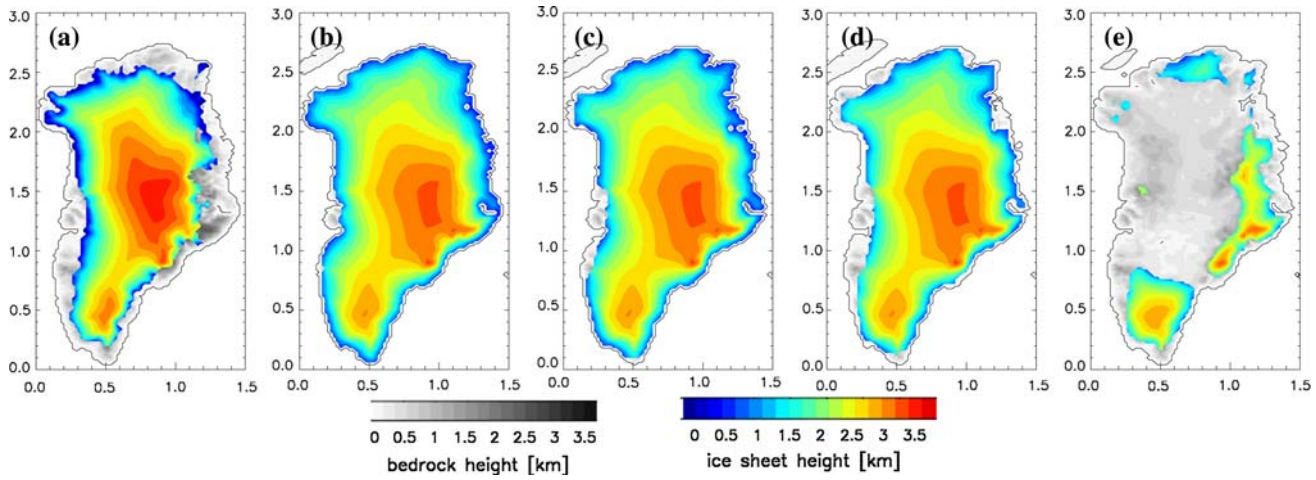

Fig. 10 **a** Greenland ice sheet geometry from observations (Bamber et al. 2001a, b). **b–e** Greenland ice sheet geometry simulated by GLIMMER using the **b** *low*, **c** *medium*, **d** *high* and **e** *very high* PDD factors, as defined in Table 2, and forced by HadCM3 pre-industrial climate

Table 3 Greenland ice-sheet volume, expressed as equivalent sea level (m), for the ice sheet simulations carried out with *low*, *medium* and *high* PDD factors

Ice sheet geometry	Observations	Low	Medium	High
Modern	7.34	9.86	9.51	8.92
$Plio^{CS}$	–	9.97	7.13	1.21
$Plio^{OS}$	–	9.64	6.93	1.16
$Plio^{CS}$–$Plio^{OS}$	–	0.33	0.20	0.057

We now move on to simulating the Pliocene ice sheets, both for the $Plio^{CS}$ and $Plio^{OS}$ cases. The results, for the *low*, *medium*, and *high* PDD factors are shown in Fig. 11, along with their corresponding differences in ice sheet thickness, $Plio^{CS}$–$Plio^{OS}$. It can be seen that the 3 degree day factors correspond to 3 different Pliocene ice sheet regimes; further sensitivity studies (not shown) indicate that there are no other stable regimes. In the $Plio^{CS}$ simulations, these correspond to equivalent sea levels of 10, 7.1, and 1.2 m (again, sumarised in Table 3). The largest of these Pliocene ice sheets is actually larger than the equivalent pre-industrial ice sheet, whereas the other two are smaller. This is most likely an indication that the *low* PDD factor is in fact too small, as it seems unlikely, on the basis of geological proxy data, that the Pliocene ice sheet should be larger than modern, and furthermore it is not consistent with estimates of global sea level change at the Pliocene relative to modern (see Sect. 3). For the other two PDD factors, they could be regarded as Early and Late Pliocene ice sheets. The ice sheet reconstructed for PRISM (which is the ice sheet in our GCM Pliocene simulations), is somewhat intermediate between the two. It is also clear that there is not a large relative difference between the $Plio^{CS}$ and $Plio^{OS}$ ice sheets, for any of the PDD factors. The ice sheet volumes differ typically by just 3–4%, corresponding to sea level changes of 30, 20, and 6 cm, for the *low*, *medium*, and *high* PDD factors respectively. However, the direction of the change is consistently such that the $Plio^{CS}$ ice sheet is larger than the $Plio^{OS}$ ice sheet. This is at least in the same direction as required by the ''Panama Hypothesis'', and means that the increase in precipitation associated with the closure of the seaway is dominating the increase in temperature.

In addition to running the ice sheet model for Greenland, we also run it for North America, using the same PDD factors. The results support the idea that the *low* PDD factor is too small, as the modern simulation develops a significant Laurentide ice sheet over much of the the Rockies (not shown), equivalent to 8 m of sea level. Seeing as the simulated pre-industrial precipitation and temperatures are in reasonably good agreement with modern observations (not shown), we also reject the *low* simulation in the North American case. The ice volumes in all the North American simulations are summarised in Table 4. Here we concentrate on the *medium* simulation, as the same broad conclusions hold for the *high* simulation. The ice sheets over North America predicted for the pre-industrial, $Plio^{OS}$ and $Plio^{CS}$ cases, and the difference $Plio^{CS}$–$Plio^{OS}$, is shown in Fig. 12. As for Greenland, the pre-industrial ice sheet extent is consistent with observations (Fulton 1995). The total ice volume is less in the Pliocene than in the pre-industrial, mainly resulting from the lack of ice in the Pliocene in the Canadian high arctic, in particular Ellesmere Island. This is supported by geological and paleontological studies (e.g. Tedford and Harington 2003; Hulbert and Harington 1999). In contrast to the Greenland simulations, the ice sheets are larger in the $Plio^{OS}$ simulation than in the $Plio^{CS}$ simulation—this is

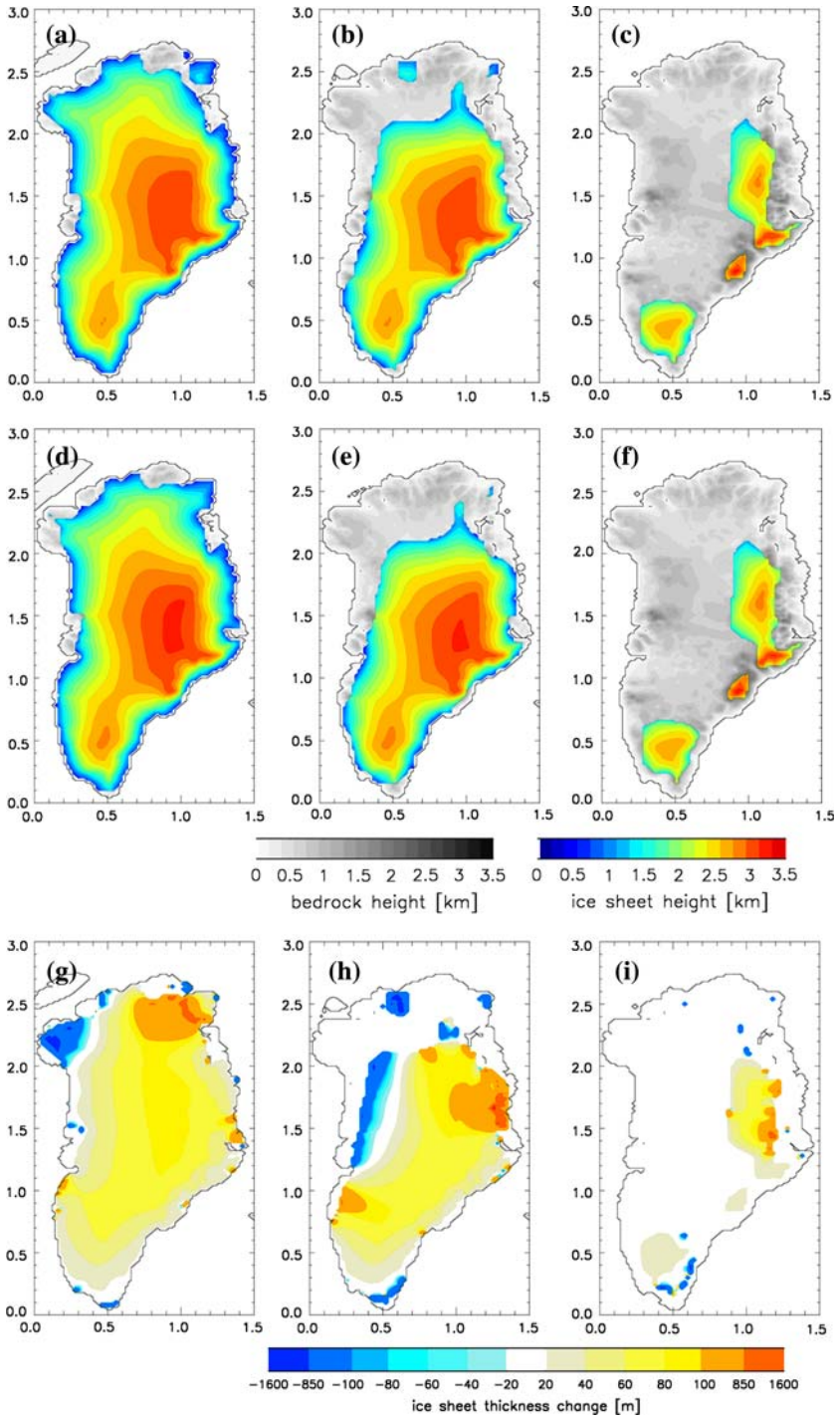

Fig. 11 **a–c** Greenland ice sheet geometry simulated by GLIMMER using the **a** *low*, **b** *medium* and **c** *high* PDD factors, as defined in Table 2, and forced by the $Plio^{OS}$ climate. **d–f** Greenland ice sheet geometry using the **d** *low*, **e** *medium* and **f** *high* PDD factors, and forced by the $Plio^{CS}$ climate. **g–i** Change in ice sheet thickness, $Plio^{CS}$–$Plio^{OS}$, for the **g** *low*, **h** *medium* and **i** *high* PDD factors

Table 4 North America ice-sheet volume, expressed as equivalent sea level (m), for the ice sheet simulations carried out with *low*, *medium* and *high* PDD factors

Ice sheet geometry	Observations	Low	Medium	High
Modern	–	7.74	0.77	0.34
$Plio^{CS}$	–	17.2	0.39	0.07
$Plio^{OS}$	–	17.5	0.53	0.08
$Plio^{CS}$–$Plio^{OS}$	–	–0.31	–0.14	–0.016

therefore in contradiction with the ''Panama Hypothesis''. However, the magnitude of change is smaller than for Greenland—14 cm in the *medium* case and 2 cm in the *high* case.

To summarise the ice sheet modelling results, we have investigated the predicted ice sheets for three distinct climate forcings—pre-industrial, $Plio^{OS}$, and $Plio^{CS}$. We have investigated the sensitivity of the predicted ice sheets to the tunable PDD factors. Based on the predicted Greenland and

North American pre-industrial ice sheets we are able to restrict the PDD factors to their *medium* and *high* values. With these PDD values, we predict Pliocene ice sheets which are smaller than pre-industrial over both Greenland and North America. The ice volume over Greenland in the $Plio^{CS}$ simulation is greater than in the $Plio^{OS}$ simulation, whereas over North America it is less. Over Greenland and North America combined, the total ice volume is greater in the closed seaway simulation than in the open seaway. This total change is consistent with the ''Panama Hypothesis''; however, the net change in sea level is small—just 6 cm in the *medium* case and 4 cm in the *high* case.

6 Discussion

There are several issues which need addressing in relation to our results, mostly related to the experimental design.

Firstly, one of the main sources of error in our results is likely due to the fact that we have made no attempt to couple the ice sheet model to the climate model, relying instead on a single iteration. Although some account is taken of the ice elevation feedback via the lapse-rate correction to the forcing climate (Eq. 2), we are neglecting other ice sheet-climate feedbacks, the strongest of which is likely related to albedo. Our ''equilibrium'' ice sheets in Figs. 11 and 12, and the corresponding ice volumes in Tables 3 and 4 should therefore primarily be considered relative to each other, rather than as ice sheets which are in equilibrium with the forcing climate. However, we do not expect this to change either the fact that the closure of the seaway led to an increase in NH ice volume, or that the increase was relatively small. It would be surprising if, in a fully coupled simulation, there was a bifurcation point lying between any of the $Plio^{CS}$ and $Plio^{OS}$ pairs in Table 3. On the other hand, such bifurcation points would certainly exist in certain special regions of parameter space; but in the ''real world'' the Earth System would move away from such regions due to, for example, changing pCO_2 or orbital configurations.

Related to this is the fact that, in our Pliocene GCM simulations, there is a significant Greenland ice sheet, albeit reduced in volume and extent relative to the present-day. This has the effect of cooling temperatures locally and most likely encouraging ice sheet inception. A perhaps cleaner experiment would have been to remove the Greenland ice sheet in the original GCM simulations, assuming that prior to the closure of the seaway, NHG was minimal. However, by removing the Greenland ice sheet in the GCM simulations, we would have lost consistency with

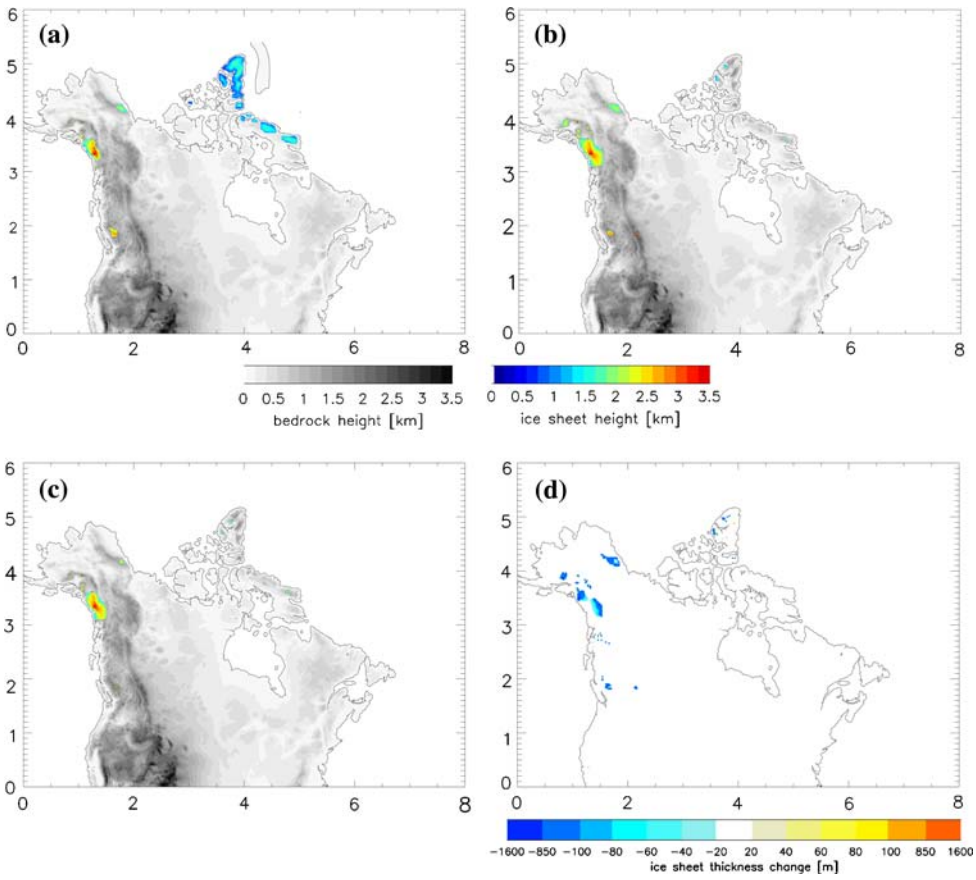

Fig. 12 **a–c** North American ice sheet geometry simulated by GLIMMER using the *medium* PDD factor, as defined in Table 2, and forced by **a** HadCM3 pre-industrial climate, **b** $Plio^{CS}$, and **c** $Plio^{OS}$. **d** Change in ice sheet thickness, $Plio^{CS}$–$Plio^{OS}$, for the *medium* PDD factor

previous simulations of the Pliocene (e.g. Haywood and Valdes 2004). This means that our ice sheet simulations are telling us more about the growth of the Greenland ice sheet subsequent to inception, rather than the inception itself. An additional apparent inconsistency is that the initial condition for all our Greenland ice sheet simulations is the present-day ice sheet of Bamber et al. (2001a, b). An alternative approach would have been to initialise with no ice sheet, or the Pliocene ice sheet which is prescribed in the GCM. Additional ice sheet simulations with varying initial conditions (not shown) indicate that, in the off-line case at least, there is no bistability with respect to initial condition. However, with the inclusion of feedbacks such as albedo and vegetation, it is likely that there would be bistability with respect to the initial ice sheet configuration.

The North American simulations do not suffer from these same drawbacks, as the GCM has no ice sheet in this region, and we initialise GLIMMER with no ice sheet. However, they do have other difficulties associated with them. Firstly, we use the modern bedrock height for the North American ice sheet simulations, and assume that this is fully relaxed. To be consistent with the actual Pliocene topography, and the GCM simulations, we could have decreased the height of the Rockies and other mountain ranges relative to modern. However, the PRISM data in this region, which is the only suitable dataset we could have used, is at a much lower spatial resolution than the ice sheet model bedrock, and so there would be inconsistencies between our pre-industrial and Pliocene ice sheet simulations. The effect of using real Pliocene bedrock height would likely be to suppress inception, but again, this would affect both Plio^{OS} and Plio^{CS} simulations, so our general conclusions are likely to be unaffected.

In this study we have not investigated the effect of varying orbital configurations on the growth of the ice sheets. In reality, the NH ice sheets would be most likely to expand during periods of low obliquity and precession, such as were manifest during the late Eemian, around 115 kyr BP. This effect was investigated by Klocker et al. (2005), who concluded that although the orbital configuration had a strong influence on NHG, it did not greatly affect the sensitivity of the system to the closure of the Panama Seaway.

The GLIMMER simulations make use of the annual PDD scheme commonly employed in ice sheet models. This effectively disregards much of the information on variability which is available from the GCM, and replaces it with a prescribed estimate of variability, which does not vary between, say, the modern and Pliocene simulations. Future studies will use a daily PDD scheme, which takes temperatures and precipitation directly from the GCM.

We have already described how the lack of coupling between the ice sheet model and the GCM leads to an underestimation of the sensitivity of the ice sheet model to the driving climates, due to the neglect of the albedo-climate feedback. However, we are also neglecting many other feedbacks. One which is likely to play an important role is that of vegetation, via the boreal forest-tundra-albedo feedback. Again, although we think that this would be an important factor to include if absolute ice sheet volumes were being predicted, or if a fully coupled transient run were to be carried out, we believe it unlikely to affect the main conclusions of this study.

There are also several issues which affect the GCM simulations, in particular the ocean component. Firstly, the oceanic initial condition for our Plio^{OS} simulation is essentially the Plio^{CS} simulation of Haywood and Valdes (2004). If the Plio^{OS} configuration were bistable, then we may be preconditioning the system into one of those stable states. A slightly more rigorous approach would be to spin up from a stable ocean state, but to properly investigate this we would have to carry out several Plio^{OS} simulations with various initial states, and look for bistability. This is impractical due to the large computational resource required. Instead, we partly justify our experimental setup by observing that apart from one study by Manabe and Stouffer (1988), there is no evidence from full complexity GCMs of bistability in the ocean, for the modern at least. In addition, the fact that we start with an Atlantic MOC which is strongly overturning, and move to a weakly overturning regime, supports the idea that the Plio^{OS} configuration also has only one stable state. Ideally, the Plio^{CS} GCM simulation should be initialised from the end of the Plio^{OS} simulation, for consistency with the direction of geological time. However, this is inpractical due to the necessity of running the simulations in series rather than in parallel, and would be inconsistent with previous work (e.g. Haywood and Valdes 2004).

Related to this is the fact that our GCM simulations are relatively short. Again, the length of the simulations is constrained by the available resource. It could be that given enough time, the system would revert into a different state, perhaps with a strongly overturing Atlantic circulation in the Plio^{OS} configuration. However, we consider this unlikely; the lack of trend in the global mean surface air temperatures, as discussed in Sect. 3, gives some confidence that the system is close to equilibrium, at least at the surface and throughout the mixed layer. However, the deep ocean temperatures in our simulations are further from equilibrium. Figure 13a shows a timeseries of the global mean deep ocean (about 2.7 km depth) temperature, for the Plio^{CS} and Plio^{OS} simulations, as well as the pre-industrial control. This shows that there are still residual trends in the deep ocean temperatures. However, they are relatively small, and the Plio^{OS} simulation, which may be expected to be furthest from equilibrium, has a similar trend to the

pre-industrial, which has a total length of over 750 years. An alternative approach would be to attempt to accelerate the convergence of the simulations, a technique employed by previous workers simulating the pre-Quaternary (e.g. Otto-Bleisner et al. 2002). However, these techniques are in general most useful in cases where the ocean circulation is completely unknown, and the ocean is initialised from a homogeneous state. In our case, it is not guaranteed that there would be a significant time-saving in accelerating the simulations, because after running in accelerated mode, a final fully-coupled phase would still need to be carried out. Specifically for this work, further confidence about the robustness of the conclusions related to the ice sheets can be found from Fig. 13b and c, which shows timeseries of the temperature and precipitation averaged over Greenland, for the Plio^{CS} and Plio^{OS} simulations. This indicates that those parameters which are important for ice sheet evolution are close to equilibrium by the end of the Plio^{CS} and Plio^{OS} simulations. Even so, long transient simulations with models of intermediate complexity (in particular with energy balance atmospheres, e.g. Bauer et al. 2004) have resulted in sudden changes in ocean circulation following periods of apparent stability in SST. This will be investigated further in the framework of a future study which will lengthen the simulations, and also investigate the sensitivity of the results to the prescribed CO_2 concentration and the orbital configuration.

In this study, we have not investigated the sensitivity of the results to the depth of the seaway in the Plio^{OS} simulation. It is likely that if the seaway were shallow enough, then the mixing of Atlantic and Pacific waters would be reduced to such an extent that the deep water formation in the high latitude Atlantic would not be suppressed, and the Plio^{OS} and Plio^{CS} simulations would not greatly differ from each other. We expect that the response to the opening/closure of the seaway is threshold-like, and once the Atlantic MOC is suppressed, further deepening would not greatly affect the circulation and climate response. However, this remains to be tested by future work.

As discussed in Sect. 4, the Plio^{CS} GCM simulation has been found to agree reasonably well with the available paleodata (Haywood and Valdes 2004; Haywood et al. 2005). Direct validation of the Plio^{OS} simulation (e.g. the surface temperature change, Plio^{CS}–Plio^{OS}, in Fig. 2), would require synchronous data from a number of sediment cores from time periods both before and after the closure of the seaway. Although some such data is available (e.g. Hodell and Kennett 1985), there is a scarcity of data which is well dated (to minimise contamination of the signal from glacial/interglacial cycles), well preserved (to minimise problems of diagenesis), and away from coastal regions with significant boundary currents (which may be influenced by local signals which are not likely to be well simulated by the model). In addition, it is difficult to relate changes in a paleoceanographic record to a specific cause, because in reality, many forcing factors (such as CO_2 concentration) will have varied over the time period considered, not just the closure of the seaway. Despite all this, here we present a brief model-data comparison of salinity changes in the Caribbean. Haug et al. (2001) and Steph et al. (2006) have analysed the $\delta^{18}O$ of *Globigerinoides sacculifer* from ODP sites 999 and 1000 respectively. Both studies suggest an increase in salinity in the Caribbean from 5.5–3.0 Ma, which they attribute to circulation and precipitation changes following the closure of the Panama Seaway. Figure 14 shows the location of these cores, along with our modelled change in salinity, Plio^{CS}–Plio^{OS}, averaged over the uppermost 110 m of the ocean, an appropriate depth for *G. sacculifer* in this region (Steph et al. 2006). Although the model shows an increase in salinity at site 999, in agreement with the data, it shows a freshening at site 1000, which is in disagreement with the data. Both comparisons are difficult to interpret, given that they are in regions of relatively steep gradients in modelled

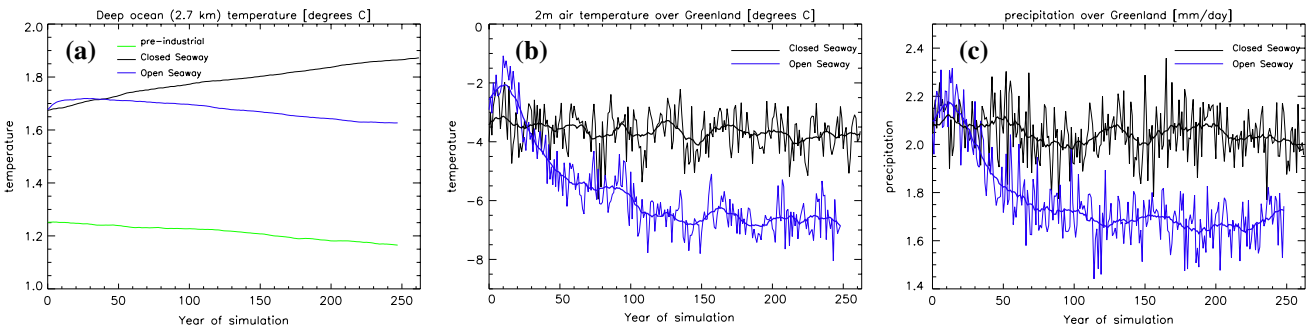

Fig. 13 Timeseries of **a** global mean deep ocean (about 2.7 km depth) temperature, **b** Greenland 2 m air temperature, and **c** Greenland precipitation, for the Plio^{OS} and Plio^{CS} simulations. **a** Also includes the pre-industrial simulation. **b** and **c** Also show the 20-year running mean with a *thick line*. Greenland is defined in this case as being between 75°W and 10°W and 58°N and 85°N

salinity change. In addition, the Caribbean is not an ideal place to carry out model-data comparison in this case. The present-day salinity in the basin is in reality influenced by flow through several narrow straits and passages (Steph et al. 2006), which are not at all resolved by the ocean model. In addition, these currents are very likely to have changed significantly due to tectonic changes over the period of interest; again, this effect is not included in our model simulations. A possible reason for the model-data disagreement at site 1000 is an oversimulation of precipitation increase in the Caribbean basin, $Plio^{CS}$–$Plio^{OS}$ (Fig. 9). This could be an indication that the changes we see in modelled Atlantic circulation are too large, *i.e.* the Atlantic ocean circulation in the $Plio^{OS}$ simulation, shown in Fig. 4b, is too weak, and not enough heat is being transported northwards. The implications of this for our ice sheet model simulations of NHG are also hard to interpret, but it is possible that a stronger overturning in the North Atlantic in the $Plio^{OS}$ simulation would lead to a climate that was more similar to that of the $Plio^{CS}$ simulations, leading to an ice volume change even smaller than that which we have simulated. Clearly, a more thorough model-data analysis needs to be carried out, in particular with data which is far from coastal regions and less influenced by local effects which are not resolved by the model. Work currently underway is attempting to provide multi-proxy estimates of North and South mid-Atlantic paleotemperatures from the appropriate time periods, in an attempt to validate the $Plio^{OS}$ in more detail (D.N. Schmidt, Earth Sciences, University of Bristol, personal communication). This will be the subject of a future study.

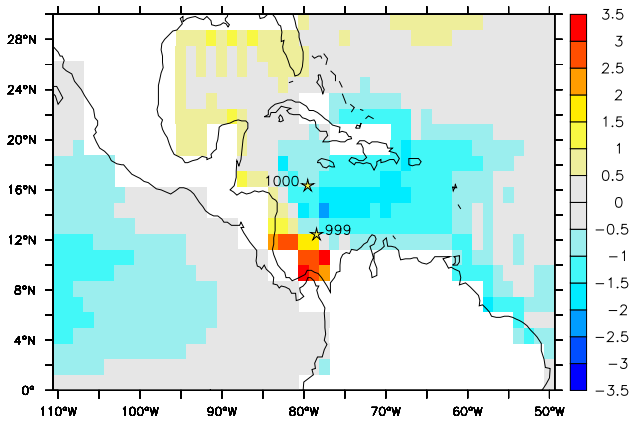

Fig. 14 Modelled change in salinity [psu], $Plio^{CS}$–$Plio^{OS}$, averaged over the uppermost 110 m of the ocean. Also shown by stars are ODP sites 999 and 1000, which have been analysed by Haug et al. (2001) and Steph et al. (2006), respectively. The *color of the stars* indicates that both sites show an increase in salinity over the period 5.5–3.0 Ma, but does not represent an actual value

7 Conclusions

We have carried out fully coupled atmosphere-ocean simulations, with a full complexity GCM and boundary conditions appropriate for the Pliocene, post and prior to the closure of the Panama Seaway. We have found that the GCM results are consistent with the ''Panama Hypothesis'', namely that with the open seaway, the mixing of Atlantic and Pacific waters reduces the salinity contrast between the two basins, leading to a reduction in deep water formation in the high latitude Atlantic and a much reduced Atlantic MOC relative to the closed seaway configuration. The closure of the seaway therefore is associated with warmer temperatures in the North Atlantic (in fact, the entire NH), greater evaporation, and greater precipitation over Greenland and North America. We address the problem of which of the warmer temperatures and increased precipitation is most important for NHG, by using a high resolution dynamical ice sheet model. The results from this indicate that the precipitation changes dominate the temperature changes, thereby further supporting the ''Panama Hypothesis''. However, we find that the associated changes in ice volume are relatively small, and equate to between 4 and 6 cm of sea level. Therefore, we can conclude that although the closure of the Panama Seaway during the Pliocene likely increased the rate of, or accelerated the initiation of, NHG, it was not a primary factor. A more likely candidate is decreasing levels of pCO_2 during the Neogene, coupled with fluctuating orbital configurations, culminating in the crossing of a critical threshold (e.g. Berger et al. 1999).

In order to more rigorously address this problem, it is necessary to carry out coupled climate-icesheet-vegetation simulations, including orbital and pCO_2 variations. This is currently not practical due to the high computational cost, but should be possible in the near future in the framework of asynchronously coupled components of the Earth system.

One additional tentative and speculative conclusion which we propose, stems from the time-varying record of ice rafted debris (IRD) in the Iceland Plateau, from ODP 907, during the Pliocene, presented by Bartoli et al. (2005). This record is interpreted as an indicator of the build up of the Greenland ice sheet, and reveals a step-wise response, with three distinct growth phases (a ''precursor'' phase followed by two main phases). It is possible that these correspond to the three Greenland ice sheet configurations in Fig. 11. Although the three modelled configurations are due to varying PDD factors, it is likely that three similar configurations would be observed with gradually cooling forcing climates. This also remains a question for future work, again in the framework of asynchronously coupled transient simulations.

Acknowledgements This work was carried out in the framework of the British Antarctic Survey GEACEP (Greenhouse to ice-house: Evolution of the Antarctic Cryosphere And Palaeoenvironment) programme. We thank three anonymous reviewers for their useful comments. Thanks to Daniela Schmidt for useful discussions concerning the paleodata.

References

Bamber JL, Layberry RL, Gogenini SP (2001a) A new ice thickness and bed data set for the Greenland ice sheet 1: Measurement, data reduction, and errors. J Geophys Res 106(D24):33773–33780

Bamber JL, Layberry RL, Gogenini SP (2001b) A new ice thickness and bed data set for the Greenland ice sheet 2: Relationship between dynamics and basal topography. J Geophys Res 106(D24):33781–33788

Barreiro M, Philander G, Pacanowski R, Fedorov A (2005) Simulations of warm tropical conditions with application to middle Pliocene atmospheres. Clim Dyn 26(4):349–365. doi:10.1007/s00382-005-0086-4

Bartoli G, Sarnthein M, Weinelt M, Erlenkeuser H, Garbe-Schonberg D, Lea W (2005) Final closure of Panama and the onset of Northern Hemisphere glaciation. Earth Planet Sci Lett 237:33–44

Bauer E, Ganopolski A, Montoya M (2004) Simulation of the cold climate event 8200 years ago by meltwater outburst from Lake Agassiz. Paleoceanography 19:PA3014

Berger A, Li XS, Loutre MF (1999) Modelling northern hemisphere ice volume over the last 3 Ma. Quat Sci Rev 18:1–11

Berggren WA, Kent DV, Swisher CC, Aubry MP (1995) A revised Cenozoic geochronology and chronostratigraphy. In: Berggren WA, Kent DV, Aubry MP, Hardenbol J (eds) Geochronology, time scales and global stratigraphic correlation, vol 54. Tulsa, Society for sedimentary geology special publication, pp 129–212

Bryan K (1969) Climate and the ocean circulation. III. The ocean model. Mon Wea Rev 97:806–827

Cattle H, Crossley J (1995) Modelling Arctic climate change. Philos Trans R Soc Lond A 352:201–213

Cox P, Betts R, Bunton C, Essery R, Rowntree PR, Smith J (1999) The impact of new land-surface physics on the GCM simulation and climate sensitivity. Clim Dyn 15:183–203

Cusack S, Slingo A, Edwards JM, Wild M (1998) The radiative impact of a simple aerosol climatology on the Hadley Centre GCM. Q J R Meteorol Soc 124:2517–2526

DeConto RM, Pollard D (2003) Rapid Cenozoic glaciation of Antarctica induced by declining atmospheric CO_2. Nature 421:245–249

Dowsett HJ, Cronin TM (1990) High eustatic sea level during the Middle Pliocene: evidence from the southeastern U.S. Atlantic Coastal Plain. Geology 18:435–438

Dowsett HJ, Barron JA, Poore RZ, Thompson RS, Cronin TM, Ishman SE, Willard DA (1999) Middle Pliocene paleoenvironmental reconstruction: PRISM2. USGS Open File Report 99-535. http://pubs.usgs.gov/of/1999/of99-535/

Edwards JM, Slingo A (1996) Studies with a flexible new radiation code 1: choosing a configuration for a large-scale model. Q J R Meteorol Soc 122:689–719

Fedorov AV, Dekens PS, McCarthy M, Ravelo AC, de Menocal PB, Barreiro M, Pacanowski RC, Philander SG (2006) The Pliocene paradox (mechanisms for a permanent El Niño). Science 312:1485–1489

Fulton RJ (1995) Surficial materials of Canada, Geological Survey of Canada, Map 1880A, scale 1:15,000,000

Gent PR, McWilliams JC (1990) Isopycnal mixing in ocean circulation models. J Phys Oceanogr 20:150–155

Gordon C, Cooper C, Senior CA, Banks H, Gregory JM, Johns TC, Mitchell JFB, Wood RA (2000) The simulation of SST, sea ice extents and ocean heat transports in a version of the Hadley Centre coupled model without flux adjustments. Clim Dyn 16:147–168

Gregory JM, Mitchell JFB (1997) The climate response to CO_2 of the Hadley Centre coupled AOGCM with and without flux adjustment. Geophys Res Lett 24:1943–1946

Gregory D, Kershaw R, Inness PM (1997) Parametrisation of momentum transport by convection II: tests in single column and general circulation models. Q J R Meteorol Soc 123:1153–1183

Hanna E, McConnell J, Das S, Cappelen J, Stephens A (2006) Observed and modeled Greenland ice sheet snow accumulation, 1958–2003, and links with regional climate forcing. J Clim 19:344–358

Haug GH, Tiedemann R (1998) Effect of the formation of the Isthmus of Panama on Atlantic Ocean thermohaline circulation. Nature 393:673–676

Haug GH, Tiedemann R, Zahn R, Ravelo AC (2001) Role of Panama uplift on oceanic freshwater balance. Geology 29:207–210

Haywood AM, Valdes PJ (2004) Modelling Middle Pliocene warmth: contribution of atmosphere, oceans and cryosphere. Earth Planet Sci Lett 218:363–377

Haywood AM, Valdes PJ, Sellwood BW (2000) Global scale palaeoclimate reconstruction of the middle Pliocene climate using the UKMO GCM: initial results. Glob Planet Change 25(1–3):239–256

Haywood AM, Dekens P, Ravelo AC, Williams M (2005) Warmer tropics during the mid Pliocene? Evidence from alkenone paleothermometry and a fully coupled ocean-atmosphere GCM. Geochem Geophys Geosyst 6(3) doi:10.1029/2004GC000799

Hibler WD (1979) A dynamic thermodynamic sea ice model. J Phys Oceanogr 9:815–846

Hodell DA, Kennett JP (1985) Miocene paleoceanography of the South Atlantic Ocean at 22, 16, and 8 Ma. In: Kennett JP (ed) The Miocene Ocean: paleoceanography and biogeography, vol 163. Geological Society of America (GSA), Boulder, pp 317–337

Hulbert RC, Harington CR (1999) An early Pliocene hipparionine horse from the Canadian Arctic. Paleontology 42:1017–1025

Huybrechts P (1996) Basal temperature conditions of the Greenland ice sheet during the glacial cycles. Ann Glaciol 23:226–236

IPCC (2001) Climate change 2001: the scientific basis. In: Houghton JT, Ding Y, Griggs DJ, Noguer M, van der Linden PJ, Xiaosu D (eds). Cambridge University Press, UK, pp 944

Keigwin LD (1982) Isotopic paleoceanography of the Caribbean and east Pacific: role of Panama uplift in late Neogene time. Science 217:350–352

Klocker A, Prange M, Schulz M (2005) Testing the influence of the Central American seaway on orbitally forced Northern Hemisphere glaciation. Geophys Res Lett 32:L03703. doi:10.1029/2004GL021564

Kürschner WM, Van der Burgh J, Visscher H, Dilcher DL (1996) Oak leaves as biosensors of late Neogene and early Pleistocene paleoatmospheric CO_2 concentrations. Mar Micropaleontol 27:299–312

Lambeck K, Nakiboglu SM (1980) Seamount loading and stress in the ocean lithosphere. J Geophys Res 85:6403–6418

Lear CH, Rosenthal Y, Wright JD (2003) The closing of a seaway: ocean water masses and global climate change. Earth Planet Sci Lett 210:425–436

Lunt DJ, de Noblet-Ducoudre N, Charbit S (2004) Effects of a melted Greenland ice sheet on climate, vegetation, and the crysophere. Clim Dyn 23(7–8):679–694

Maier-Reimer E, Mikolajewicz U, Crowley T (1990) Ocean general circulation model sensitivity experiment with an open Central American Isthmus. Paleoceanography 5:349–366

Manabe S, Stouffer RJ (1988) Two stable equilibria of a coupled ocean-atmosphere model. J Clim 1:841–866

Marshall LG, Webb SD, Sepkoski JJ, Raup DM (1982) Mammalian evolution and the great american interchange. Science 215:1351–1357

Maslin MA, Li XS, Loutre MF, Berger A (1998) The contribution of orbital forcing to the progressive intensification of Northern Hemisphere glaciation. Quat Sci Rev 17:411–426

Mikolajewicz U, Crowley TJ (1997) Response of a coupled ocean/energy balance model to restricted flow through the Central American Isthmus. Paleoceanography 12:429–441

Mikolajewicz U, Maier-Reimer E, Crowley T, Kim KY (1993) Effect of Drake and Panamanian Gateways on the circulation of an ocean model. Paleoceanography 8:409–426

Murdock TQ, Weaver AJ, Fanning AF (1997) Paleoclimatic response of the closing of the Isthmus of Panama in a coupled ocean-atmosphere model. Geophys Res Lett 24:253–256

Nisancioglu KH, Raymo ME, Stone PH (2003) Reorganization of Miocene deep water circulation in response to the shoaling of the Central American Seaway. Paleoceanography 18:1006. doi:10.1029/2002PA000767

Otto-Bliesner BL, Brady EC, Shields C (2002) Late Cretaceous ocean: coupled simulations with the National Center for Atmospheric Research Climate System Model. J Geophys Res 107(D2):4019. doi:10.1029/2001JD000821

Payne AJ (1999) A thermomechanical model of ice flow in West Antarctica. Clim Dyn 15:115-125

Philander GS, Fedorov AV (2003) Role of tropics in changing the response to Milankovich forcing some three million years ago. Paleoceanography 18. doi:10.1029/2002PA000837

Peixoto JP, Oort AH (1992) Physics of climate. Springer, New York, pp 345

Pollard D, Thompson SL (1997) Driving a high-resolution dynamic ice sheet model with GCM climate: ice-sheet initiation at 116,000 BP. Ann Glaciol 25:296–304

Prange M, Schulz M (2004) A coastal upwelling seesaw in the Atlantic Ocean as a result of the closure of the Central American Seaway. Geophys Res Lett 31:L17207. doi:10.1029/2004GL020073

Prange M, Schulz M (2006) Panamanian gateway closure chilled North America: a dynamical impact of the atmosphere on Northern Hemisphere glaciation. Geophysical Research Abstracts, 8, EGU—3rd General Assembly, Vienna

Ravelo AC, Andreasen DH, Lyle M, Lyle AO, Wara MW (2004) Regional climate shifts caused by gradual global cooling in the Pliocene epoch. Nature 42:263–267

Ravelo AC, Dekens PS, McCarthy M (2006) Evidence for El Nino-like conditions during the Pliocene. GSA Today 16:4–11

Raymo ME (1994) The initiation of Northern Hemisphere glaciation. Annu Rev Earth Planet Sci 22:353–383

Raymo ME, Grant B, Horowitz M, Rau GH (1996) Mid-Pliocene warmth: stronger greenhouse and stronger conveyor. Mar Micropaleontol 27:313–326

Rea DK, Snoeckx H, Joseph LH (1998) Late Cenozoic Eolian deposition in the North Pacific: Asian drying, Tibetan uplift, and cooling of the Northern Hemisphere. Paleoceanography 13:215–224

Reeh (1991) Parameterization of melt rate and surface temperature on the Greenland ice sheet. Polarforschung 59/3:113–128

Schmidt DN (2007) The closure history of the Panama Isthmus: evidence from isotopes and fossils to models and molecules. In: Williams M, Haywood AM, Gregory JF, Schmidt DN (eds) Deep time perspectives on climate change—marrying the signal from computer models and biological proxies. Geological Society of London, London (in press)

Schneider B, Schmittner A (2006) Simulating the impact of the Panamanian seaway closure on ocean circulation, marine productivity and nutrient cycling. Earth Planet Sci Lett 246:367–380

Shackleton NJ, Le J, Mix A, Hall MA (1992) Carbon isotope records from Pacific surface waters and atmospheric carbon dioxide. Quat Sci Rev 11:387–400

Steph S, Tiedemann R, Prange M, Groenveld J, Nurnberg D, Reuning L, Schulz M, Haug GH (2006) Changes in Caribbean surface hydrography during the Pliocene shoaling of the Central American Seaway. Paleoceanography 21:PA4221. doi:10.1029/2004PA001092

Tedford RH, Harington CR (2003) An Arctic mammal fauna from the Early Pliocene of North America. Nature 425:388–390

US Department of Commerce, National Oceanic and Atmospheric Administration, National Geophysical Data Center (2001) 2-minute Gridded Global Relief Data (ETOPO2). http://www.ngdc.noaa.gov/mgg/fliers/01mgg04.html

Van der Burgh J, Visscher H, Dilcher DL, Kürschner WM (1993) Paleoatmospheric signatures in Neogene fossils leaves. Science 260:1788–1790

Von der Heydt A, Dijkstra HA (2005) Flow reorganizations in the Panama Seaway: a cause for the demise of Miocene corals? Geophys Res Lett 32:2, Art. No. L02609. doi:10.1029/2004GL020990